Decay modes of two repulsively interacting bosons

2011 J. Phys. B: At. Mol. Opt. Phys. 44 195301

(http://iopscience.iop.org/0953-4075/44/19/195301)

J. Phys. B: At. Mol. Opt. Phys. **44** (2011) 195301 (8pp) doi:10.1088/0953-4075/44/19/195301

Decay modes of two repulsively interacting bosons

Sungyun Kim[1] **and Joachim Brand**[2]

[1] Hoseo University, 165 Sechul Li, Baebang Myun, Asan, Chungnam 336-795, Korea
[2] Centre for Theoretical Chemistry and Physics, New Zealand Institute for Advanced Study, Massey University, Private Bag 102904, North Shore, Auckland 0745, New Zealand

E-mail: rdecay@googlemail.com and J.Brand@massey.ac.nz

Received 29 June 2011, in final form 5 August 2011
Published 1 September 2011
Online at stacks.iop.org/JPhysB/44/195301

Abstract
We study the decay of two repulsively interacting bosons tunnelling through a delta potential barrier by a direct numerical solution of the time-dependent Schrödinger equation. The solutions are analysed according to the regions of particle presence: both particles inside the trap (in–in), one particle in and one particle out (in–out) and both particles outside (out–out). It is shown that the in–in probability is dominated by the exponential decay, and its decay rate is predicted very well from outgoing boundary conditions. Up to a certain range of interaction strength, the decay of in–out probability is dominated by the single-particle decay mode. The decay mechanisms are adequately described by simple models.

(Some figures in this article are in colour only in the electronic version)

1. Introduction

The decay of a particle by tunnelling through a potential barrier into a continuum is a fundamental and unique phenomenon in quantum mechanics. The tunnelling of multi-particle systems is just as important and presents one of the places where the understanding of macroscopic quantum phenomena can start [1]. The tunnelling and decaying of Bose–Einstein condensates (BECs) are attractive subjects of study [2], since the BEC is a unique state of matter where quantum mechanical features are manifested at the macroscopic level. After BECs were first realized experimentally in dilute atomic gases [3], a huge amount of related research followed. Ultra-cold atoms are usually trapped in a finite potential well and the decay by tunnelling into a continuum is an existing and potentially desirable possibility. In this context, it was realized that understanding the decay dynamics by tunnelling is a very important task [4, 5].

In most cases, BECs have thousands to millions of particles and the dynamics is adequately described by the Gross–Pitaevskii (GP) equation [6, 7] of mean-field theory [8], a nonlinear Schrödinger equation. The GP equation governs the time evolution of the phase and particle number density of an essentially fully Bose-condensed system. With many works on the mean-field description of BEC tunnelling [9–13], it is remarkable that there is still a discussion, both about the technical implementation [12] and the correct formulation of mean-field theory related to the decay problem [10]. It is thus desirable to obtain a detailed understanding of the microscopic physics of the multi-particle decay.

The cases of stronger interactions or fewer particle numbers are also important, where the GP equation is less accurate. In the few boson regime, the correlated decay of particles was observed and studied both experimentally and theoretically [14, 15]. The particle correlation in the decayed wave is important in relation to the atom laser [16]. For strongly interacting bosons in a one-dimensional trap, Bose condensation is not relevant but the gas acquires properties related to fermionic systems [17]. In the Tonks–Girardeau limit of infinite interactions the few boson decay problem was treated analytically [18], and numerical simulation has addressed the crossover for finite interactions from a harmonic trap with up to four bosons [19]. The analytic treatment of a few boson decays with finite interaction strength remains a difficult task.

In this paper, we approach this problem both numerically and analytically. We study the simplest case of two repulsively interacting bosons in a potential trap in one dimension. The time evolution of the decay is obtained from first principles by solving the time-dependent Schrödinger equation numerically.

Then, it is compared to approximate analytic methods, starting from the exact solutions of local spatial regions. The decay phenomena are investigated for a wide range of interaction strength, from zero to very strong repulsion. The analytic model predicts an exponential decay mode of the interacting system, which is in very good agreement with our numerical simulation. Also, the decay of the total particle number is well explained with a simple theoretical model.

2. The model Hamiltonian

We choose a model Hamiltonian for the two interacting boson decays. Considering the kinetic energy, external potential $\tilde{V}_{\rm ex}$ for trapping and interaction $\tilde{U}$ between bosons, the total Hamiltonian with two identical bosons is written as

$$\tilde{H} = -\frac{\hbar^2}{2m}\frac{\partial^2}{\partial \tilde{x}_1^2} - \frac{\hbar^2}{2m}\frac{\partial^2}{\partial \tilde{x}_2^2} + \tilde{V}_{\rm ex}(\tilde{x}_1) + \tilde{V}_{\rm ex}(\tilde{x}_2) + \tilde{U}(\tilde{x}_1, \tilde{x}_2). \tag{1}$$

The external potential is

$$\tilde{V}_{\rm ex}(\tilde{x}) = \begin{cases} \infty & \text{for } \tilde{x} < 0 \\ \tilde{V}\delta(\tilde{x} - L) & \text{for } \tilde{x} \geqslant 0, \end{cases} \tag{2}$$

and it acts as a potential trap by a delta barrier at position L. This choice of external potential has some advantages in that the delta barrier has zero width so the consideration of the decay process inside the barrier is not needed. Also, the analytical treatment of the decay process is simplified. In a single-particle case, we found that the exponential decay mode dominates and non-exponential features are strongly suppressed compared to a finite-width barrier case. Computationally, the narrow width of the delta function makes the Hamiltonian matrix more sparse, which makes the problem tractable.

Considering only s-wave scattering [2], the interaction potential between particles 1 and 2 is given as

$$\tilde{U}(\tilde{x}_1, \tilde{x}_2) = \tilde{g}\delta(\tilde{x}_1 - \tilde{x}_2), \tag{3}$$

where $\tilde{g}$ is a coupling constant and $\tilde{x}_1$ and $\tilde{x}_2$ are the positions of each boson, respectively.

To simplify the analysis and compare the result with external parameters, we introduce dimensionless units. The new length unit x is defined as $x \equiv \tilde{x}/L$. The Hamiltonian is rewritten as

$$\tilde{H} = -\frac{\hbar^2}{2mL^2}\frac{\partial^2}{\partial x_1^2} - \frac{\hbar^2}{2mL^2}\frac{\partial^2}{\partial x_2^2} + \frac{\tilde{V}}{L}\delta(x_1 - 1) + \frac{\tilde{V}}{L}\delta(x_2 - 1) + \frac{\tilde{g}}{L}\delta(x_1 - x_2), \quad \text{for } x \geqslant 0. \tag{4}$$

Dividing both sides by $\hbar^2/(mL^2)$, we obtain the rescaled, dimensionless Hamiltonian $H \equiv mL^2\tilde{H}/\hbar^2$:

$$H = -\frac{1}{2}\frac{\partial^2}{\partial x_1^2} - \frac{1}{2}\frac{\partial^2}{\partial x_2^2} + V\delta(x_1 - 1) + V\delta(x_2 - 1) + g\delta(x_1 - x_2). \tag{5}$$

Here,

$$V \equiv \frac{mL}{\hbar^2}\tilde{V}, \qquad g \equiv \frac{mL}{\hbar^2}\tilde{g}. \tag{6}$$

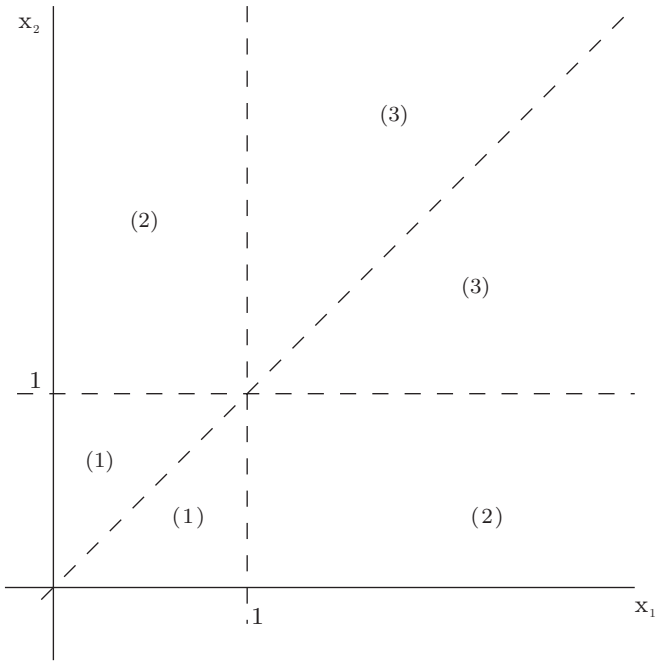

Figure 1. Hamiltonian in x_1–x_2 space.

The Schrödinger equation with this Hamiltonian is given by

$$\mathrm{i}\partial_t\psi = H\psi, \tag{7}$$

where $t = \hbar\tilde{t}/(mL^2)$ with $\tilde{t}$ being unscaled time.

In x_1–x_2 space, the Hamiltonian looks like figure 1. The dotted lines represent delta potentials from the trap and interaction between the particles. From now on, we denote the region where both particles are inside the trap as region (1), where one particle is in and one particle is out of the trap as region (2) and where both particles are out of the trap as region (3).

3. Numerical simulation of the two boson decay

Now, we set up the decay of two interacting identical bosons in this Hamiltonian. We choose the initial condition that both particles are inside the delta trap as the two boson ground states of the $V \to \infty$ case. Specifically, this initial state $\psi_{\rm ini}(x_1, x_2)$ is given by [20]

$$\psi_{\rm ini}(x_1, x_2) = N_{\rm ini}((A_1(k_{1i}, k_{2i})\,\mathrm{e}^{\mathrm{i}k_{1i}x_1} - A_2(k_{1i}, k_{2i})\,\mathrm{e}^{-\mathrm{i}k_{1i}x_1})\sin(k_{2i}x_2) + (A_3(k_{1i}, k_{2i})\,\mathrm{e}^{\mathrm{i}k_{2i}x_1} - A_4(k_{1i}, k_{2i})\,\mathrm{e}^{-\mathrm{i}k_{2i}x_1})\sin(k_{1i}x_2)) \quad \text{for } 0 \leqslant x_2 \leqslant x_1 \leqslant 1 \tag{8}$$

with

$$A_1(k_1, k_2) = (\mathrm{i}k_1 + \mathrm{i}k_2 + g)(\mathrm{i}k_1 - \mathrm{i}k_2 + g), \tag{9}$$

$$A_2(k_1, k_2) = (\mathrm{i}k_1 - \mathrm{i}k_2 - g)(\mathrm{i}k_1 + \mathrm{i}k_2 - g), \tag{10}$$

$$A_3(k_1, k_2) = (\mathrm{i}k_1 + \mathrm{i}k_2 + g)(\mathrm{i}k_1 - \mathrm{i}k_2 - g) \text{ and} \tag{11}$$

$$A_4(k_1, k_2) = (\mathrm{i}k_1 + \mathrm{i}k_2 - g)(\mathrm{i}k_1 - \mathrm{i}k_2 + g). \tag{12}$$

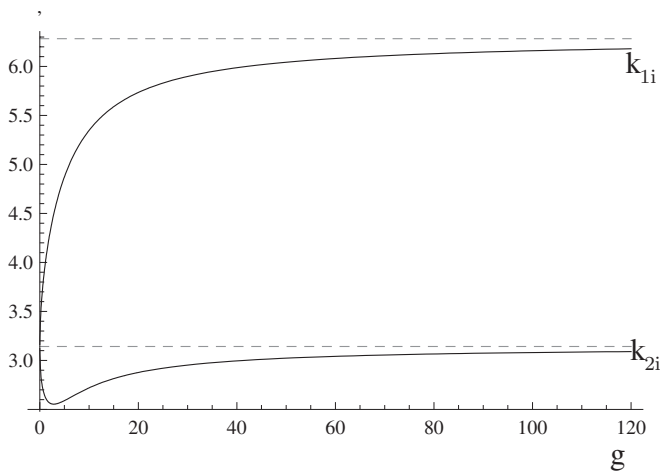

Figure 2. k_{1i} and k_{2i} versus the g plot. The dashed lines are π and 2π, the wavevectors of $V = \infty$ are the lowest and next lowest states. As the interaction strength g increases, k_{1i} approaches 2π and k_{2i} approaches π.

The initial state wavevectors k_{1i} and k_{2i} satisfy the following equations

$$k_{1i} = \pi + \arctan\left(\frac{g}{k_{1i} - k_{2i}}\right) + \arctan\left(\frac{g}{k_{1i} + k_{2i}}\right), \tag{13}$$

$$k_{2i} = \pi - \arctan\left(\frac{g}{k_{1i} - k_{2i}}\right) + \arctan\left(\frac{g}{k_{1i} + k_{2i}}\right). \tag{14}$$

The initial wavefunction in the $0 \leqslant x_1 \leqslant x_2 \leqslant 1$ region is obtained from the boson symmetry condition $\psi_{\rm ini}(x_1, x_2) = \psi_{\rm ini}(x_2, x_1)$. In other regions the initial wavefunction is zero. The normalization constant $N_{\rm ini}$ is chosen to satisfy $\int {\rm d}x_1\, {\rm d}x_2 |\psi_{\rm ini}|^2 = 1$. k_{1i} and k_{2i} versus interaction strength g is shown in figure 2. For zero interaction both k_{1i} and k_{2i} are the same as π, the single-particle ground-state wavevector. For nonzero g they rapidly deviate from π as g increases, and k_{1i} approaches 2π and k_{2i} approaches π (figure 2).

To analyse the decay of interacting bosons, we solve the Schrödinger equation directly. The Schrödinger equation and its formal solution are

$$i\partial_t \psi = H\psi \tag{15}$$

$$\psi(t) = \exp(-iHt)\psi(0). \tag{16}$$

We use the Crank–Nicolson method to solve this equation numerically [21, 22].

For the numerical representation of the Hamiltonian, we choose the triangular region $0 \leqslant x_2 \leqslant x_1 \leqslant X_{\rm max}$ in x space (the $0 \leqslant x_1 \leqslant x_2 \leqslant X_{\rm max}$ region is determined due to the bosonic symmetry), with $X_{\rm max}$ being large enough that in our observing time very little decay products reach near $X_{\rm max}$. This region is discretized by dividing $X_{\rm max}$ by N_x, and all points in the triangular region are arranged in one column vector. The Hamiltonian matrix obtained by the discretization of x space and using a finite-difference formula for the second derivatives can be quite large, but it is a sparse matrix as most elements are zero.

For small ${\rm d}t$,

$$\exp(iH\,{\rm d}t/2)\psi(t + {\rm d}t) = \exp(-iH\,{\rm d}t/2)\psi(t) \tag{17}$$

$$\psi(t + {\rm d}t) = (1 + iH\,{\rm d}t/2)^{-1}(1 - iH\,{\rm d}t/2)\psi(t) + O({\rm d}t^3). \tag{18}$$

This method is of second order in ${\rm d}t$ and unitary (i.e. probability is conserved). This is an implicit method, since it contains the inverse operator. The matrix inversion is efficiently implemented by solving the linear equation. The time evolution of the wavefunction is obtained by iterating equation (18).

For the simulations in the next sections, the following parameters are used. $X_{\rm max} = 45$, $\Delta x = (X_{\rm max}/N_x) = 1/24$, ${\rm d}t = 0.002$, $V = 5$. The convergence of the numerical solutions is checked by changing spatial grid size and time step. We also check numerical simulations with known analytic solutions for special cases $g = 0$ and ∞. To see the effect from the reflection of waves at the boundary, the results are examined by changing $X_{\rm max}$ and by putting absorbing potentials near $X_{\rm max}$. In our parameter regime, those effects are very small and do not change the main results.

4. Results and analysis

To understand the decay of two interacting bosons, a good starting point is the parameter region where we know the exact analytic solutions. In our case, we know exact eigenfunctions of the Hamiltonian for two extreme cases, $g = 0$ and ∞. In those cases, the two-particle eigenfunctions are obtained by the combination of one-particle eigenfunctions, which are known in an analytic form. For arbitrary $g > 0$, the results lie between these two extremes, and the exact analytic forms are not known.

4.1. Vanishing and infinite interaction limits

When $g = 0$ there is no interaction between two particles. They act independently, with only a symmetric wavefunction condition. The eigenfunction is written as

$$\psi(k_1, k_2, x_1, x_2) = \tfrac{1}{\sqrt{2}}(\phi(k_1, x_1)\phi(k_2, x_2) + \phi(k_2, x_1)\phi(k_1, x_2)), \tag{19}$$

where the total eigenenergy is $E = \left(k_1^2 + k_2^2\right)/2$, and $\phi(k, x)$ is the one-particle eigenfunction with eigenwavevector k. In our model, the explicit form of ϕ is given by

$$\phi(k, x) = \begin{cases} c_1(k)\sin(kx) & \text{for } 0 < x < 1 \\ c_2(k)\,{\rm e}^{ikx} + c_3(k)\,{\rm e}^{-ikx} & \text{for } 1 \leqslant x, \end{cases} \tag{20}$$

where

$$c_1(k) = \sqrt{\frac{2}{\pi}}\frac{1}{\sqrt{1 + \frac{4V}{k}\sin k\cos k + \frac{4V^2}{k^2}\sin^2 k}}, \tag{21}$$

$$c_2(k) = \frac{1}{2}\left(-\left(i + \frac{V}{k}\right) + \frac{V}{k}\,{\rm e}^{-2ik}\right)c_1(k), \tag{22}$$

$$c_3(k) = \frac{1}{2}\left(\left(i - \frac{V}{k}\right) + \frac{V}{k}\,{\rm e}^{2ik}\right)c_1(k). \tag{23}$$

The one-particle decay rate can be calculated by the outgoing boundary condition, setting the coefficient of the outgoing wave $c_3(k) = 0$ and solving for k (this is also the pole of the scattering matrix). The equation $c_3(k) = 0$ has complex solutions, each of them corresponds to different decay modes. We denote the complex solutions of $c_3(k) = 0$ as $k_{z0}, k_{z1}, \ldots$, with k_{z0} being the lowest decay mode and k_{z1} the next lowest decay mode, etc. For the $V = \infty$ ground-state initial condition

$$\psi_{\rm ini}(x) = \sqrt{2}\sin(\pi x), \tag{24}$$

the dominant decay mode is k_{z0}. Since the decay mode wavefunction is also a complex eigenfunction, its time dependence is given by $\mathrm{e}^{-\mathrm{i}Et}$, where $E = k_{z0}^2/2$. The time evolution of one-particle probability inside the potential trap $P_{\rm 1in}(t)$ follows the exponential decay:

$$P_{\rm 1in}(t) \approx |\mathrm{e}^{-\mathrm{i}Et}|^2 = \mathrm{e}^{-\gamma_{z0}t}, \tag{25}$$

$$\gamma_{z0} = -2k_{z0r}k_{z0i}, \tag{26}$$

where k_{z0r} and k_{z0i} are the real and imaginary parts of k_{z0}, respectively.

The decay of two interacting bosons in the special cases of $g = 0$ and ∞ is obtained from the single-particle decay patterns, respectively.

For $g = 0$, the two-particle wavefunction is the product of one-particle wavefunctions, and their decay is just the product of the individual decay. With the condition that the initial wavefunction was the ground state of $V = \infty$:

$$\psi_{\rm ini}(x_1, x_2) = 2\sin(\pi x_1)\sin(\pi x_2). \tag{27}$$

If we write the probability of both particles inside the trap as P_1, the probability of one particle in and one out as P_2 and both particles out as P_3, their dominant time evolutions are

$$P_1(t) \approx \mathrm{e}^{-2\gamma_{z0}t}, \tag{28}$$

$$P_2(t) \approx 2\,\mathrm{e}^{-\gamma_{z0}t}(1 - \mathrm{e}^{-\gamma_{z0}t}), \tag{29}$$

$$P_3(t) \approx (1 - \mathrm{e}^{-\gamma_{z0}t})^2. \tag{30}$$

Another case where we know the exact eigenfunction of the Hamiltonian is the $g = \infty$ case. In this case, the two-particle eigenfunction is written as

$$\psi(k_1, k_2, x_1, x_2) = \tfrac{1}{\sqrt{2}}(\phi(k_1x_1)\phi(k_2x_2) - \phi(k_2x_1)\phi(k_1x_2)), \quad \text{for } x_1 \leqslant x_2, \tag{31}$$

and $\psi(k_1, k_2, x_1, x_2) = \psi(k_1, k_2, x_2, x_1)$ for the $x_1 < x_2$ region. Like in the case of fermions the probability density is zero along the $x_1 = x_2$ line. The $V_0 = \infty$ ground-state initial condition is given by

$$\psi_{\rm ini}(x_1, x_2) = \sqrt{2}(\sin(\pi x_1)\sin(2\pi x_2) - \sin(2\pi x_1)\sin(\pi x_2)) \quad \text{for } x_1 \geqslant x_2, \tag{32}$$

and $\psi_{\rm ini}(x_2, x_1) = \psi_{\rm ini}(x_1, x_2)$ for $x_1 < x_2$. The decay of two bosons at $g = \infty$ involves two different decay modes, with the lowest wavevector k_{z0} and the next lowest one k_{z1}. The time evolutions of P_1, P_2 and P_3 are

$$P_1(t) \approx \mathrm{e}^{-(\gamma_{z0}+\gamma_{z1})t} \tag{33}$$

$$P_2(t) \approx \mathrm{e}^{-\gamma_{z0}t}(1 - \mathrm{e}^{-\gamma_{z1}t}) + \mathrm{e}^{-\gamma_{z1}t}(1 - \mathrm{e}^{-\gamma_{z0}t}) \tag{34}$$

$$P_3(t) \approx (1 - \mathrm{e}^{-\gamma_{z0}t})(1 - \mathrm{e}^{-\gamma_{z1}t}), \tag{35}$$

with

$$\gamma_{z_j} = -2k_{zjr}k_{zji} \tag{36}$$

and k_{zjr} and k_{zji} are the real and imaginary parts of k_{zj}, respectively.

4.2. *The arbitrary $g > 0$ case*

For the general case of $0 < g < \infty$ exact analytic eigenfunctions are not known. We use the numerical method of section 3 to obtain the decay of probabilities. To conduct the simulation, first the initial condition was chosen as the ground state of the trap potential strength $V = \infty$ limit.

Quite interestingly, the numerical results in this section show that a rather simple model can be used to explain the interacting boson decay. For the decay of interacting particles, it is expected that the number density of particles shows non-exponential decay. When there are more particles inside the trap it decays faster, and with less particles the decay is slower. But if we examine the probability P_1 of both particles inside and the probability P_2 of one particle inside and another out separately, they show quite distinctive features.

If we plot the logarithm $\ln P_1$ versus time for various interaction strength g, the graphs show straight lines, meaning the decay is exponential. Furthermore, the decay rate can be obtained by theoretical estimation. Like the decay rate calculation of the one-particle case, we can apply the outgoing boundary condition for the wavefunction in region (1). Since the probability of both particles escaping simultaneously is very small due to the repulsive interaction, it is ignored. Then, the outgoing boundary condition from region (1) to region (2) can be written as follows.

First, the wavefunction in region (1) $\psi_{(1)}$, satisfying the Bethe ansatz and the boundary conditions at $x_1 = 0$ and $x_1 = x_2$, can be written as (the form of the coefficients without normalization is given in equations (9)–(12))

$$\psi_{(1)}(x_1, x_2) = (A_1(k_1, k_2)\,\mathrm{e}^{\mathrm{i}k_1x_1} - A_2(k_1, k_2)\,\mathrm{e}^{-\mathrm{i}k_1x_1})\sin(k_2x_2) + (A_3(k_1, k_2)\,\mathrm{e}^{\mathrm{i}k_2x_1} - A_4(k_1, k_2)\,\mathrm{e}^{-\mathrm{i}k_2x_1})\sin(k_1x_2), \quad \text{for } 0 \leqslant x_2 \leqslant x_1 \leqslant 1 \tag{37}$$

and the outgoing eigenfunction in region (2), $\psi_{(2)}$, can be written as

$$\psi_{(2)}(x_1, x_2) = B_1\,\mathrm{e}^{\mathrm{i}k_1x_1}\sin(k_2x_2) + B_2\,\mathrm{e}^{\mathrm{i}k_2x_1}\sin(k_1x_2), \quad \text{for } 1 < x_1, 0 \leqslant x_2 < 1 \tag{38}$$

with the boundary condition

$$\psi_{(1)}(1, x_2) = \psi_{(2)}(1, x_2), \tag{39}$$

$$\partial_{x_1}\psi_{(2)}(1, x_2) - \partial_{x_1}\psi_{(1)}(1, x_2) = 2V\psi_{(1)}(1, x_2). \tag{40}$$

Conditions (39) and (40) yield four equations with four unknowns B_1, B_2, k_1 and k_2. Solving for k_1 and k_2 we obtain two equations

$$A_1(k_1, k_2)\,\mathrm{e}^{\mathrm{i}k_1} - A_2(k_1, k_2)\,\mathrm{e}^{-\mathrm{i}k_1} = -\frac{\mathrm{i}k_1}{V}A_2(k_1, k_2)\,\mathrm{e}^{-\mathrm{i}k_1} \tag{41}$$

$$A_3(k_1, k_2)\,\mathrm{e}^{\mathrm{i}k_2} - A_4(k_1, k_2)\,\mathrm{e}^{-\mathrm{i}k_2} = -\frac{\mathrm{i}k_2}{V}A_4(k_1, k_2)\,\mathrm{e}^{-\mathrm{i}k_2} \tag{42}$$

and two complex wavevectors k_{1g} and k_{2g} for their solutions. When we write the real and imaginary parts of complex eigenvectors as $k_{1g} = k_{1gr} + \mathrm{i}k_{1gi}$ and $k_{2g} = k_{2gr} + \mathrm{i}k_{2gi}$, both of their imaginary numbers are negative. Considering that the time evolution of an energy eigenfunction follows $\mathrm{e}^{-\mathrm{i}Et}$ like the one-particle decay mode, it can be expected that

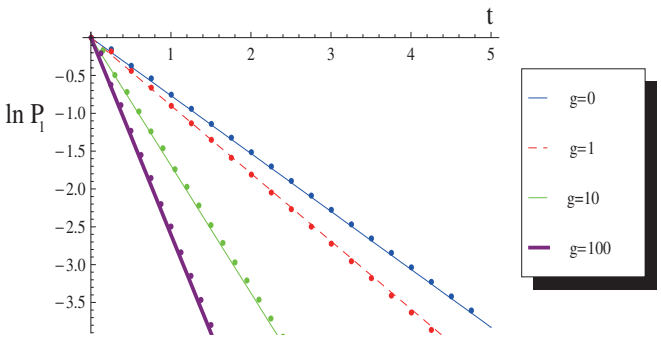

Figure 3. ln $P_1(t)$ plots for various g (different colors). Dots are from numerical simulation and lines are from theoretical prediction of decay rate by outgoing boundary conditions of (41) and (42). The numerical simulation and theoretical prediction show very good agreement.

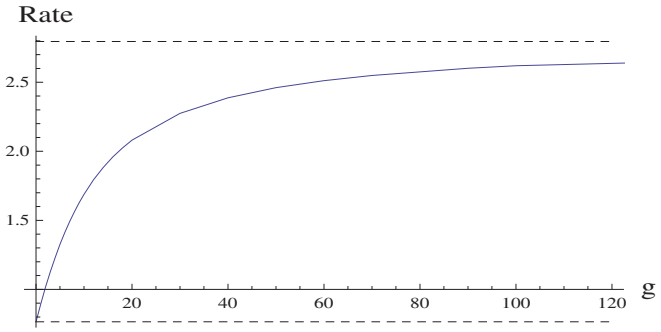

Figure 4. P_1 decay rate γ_g versus g plots. The solid line represents γ_g, lower and upper dashed lines represent P_1 decay rates of $g = 0$ and ∞ cases, respectively.

$\exp\left(-\mathrm{i}\left(k_{1g}^2 + k_{2g}^2\right)t/2\right)$ dominates in time evolution. When we compare the probability of both particles inside $P_1(t)$ with $\left|\exp\left(-\mathrm{i}\left(k_{1g}^2 + k_{2g}^2\right)t/2\right)\right|^2$, indeed we see that this is what happens. Both are in very good agreement as shown in figure 3. $P_1(t)$ decays exponentially with the decay rate predicted by the outgoing boundary conditions:

$$P_1(t) \approx \left|\exp\left(-\mathrm{i}\left(k_{1g}^2 + k_{2g}^2\right)t/2\right)\right|^2 = \mathrm{e}^{-\gamma_g t}, \tag{43}$$

$$\gamma_g = -2k_{1gr}k_{1gi} - 2k_{2gr}k_{2gi}. \tag{44}$$

Figure 4 shows that γ_g changes for various g. γ_g changes a lot for small g and approaches to the decay rate of $g = \infty$ slowly. Figure 3 shows the comparison between the $-\gamma_g t$ line from theoretical prediction and log P_1 from numerical simulation. They match very well for all $g > 0$, thus showing P_1 decays exponentially even with the interaction between bosons. Next, we consider the time evolution of P_2, one particle in and one particle out of the trap probability. It is more complicated than that of P_1, since it contains probability inflow from region (1) and outflow into region (3). Like the P_1 case, we already know the dominant parts of $P_2(t)$ for special cases, $g = 0$ and ∞.

For $g = 0$, the decay of $P_2(t)$ has the form

$$P_{2,g=0}(t) \approx 2\,\mathrm{e}^{-\gamma_{z0}t}(1 - \mathrm{e}^{-\gamma_{z0}t}) = 2\,\mathrm{e}^{-\gamma_{z0}t} - 2\,\mathrm{e}^{-2\gamma_{z0}t} \tag{45}$$

and for $g = \infty$,

$$P_{2,g=\infty}(t) \approx \mathrm{e}^{-\gamma_{z0}t}(1 - \mathrm{e}^{-\gamma_{z1}t}) + \mathrm{e}^{-\gamma_{z1}t}(1 - \mathrm{e}^{-\gamma_{z0}t}), \tag{46}$$

where γ_{z0}, and γ_{z1} are the lowest and the next lowest decay rates of one particle in the potential trap. For the $g = 0$ case, both bosons decay from the same mode independently. For the $g = \infty$ case, two bosons decay from the separate decay modes without interfering since they are almost orthogonal. For general $0 < g < \infty$, the time evolution of $P_2(t)$ will be between (45) and (46) and as g is increased $P_2(t)$ will change from (45) to (46). We try different models for two regimes where g is not large (weak or moderate repulsion) and where g is very large (strong repulsion) and investigate regions of validity for each model.

For the weak repulsive interaction, we try a simple model for P_2 decay. If we assume that the probability of both particles escaping simultaneously is very small, which is satisfied when the decay rate is small and the interparticle interaction is repulsive, then the inflow from region (1) has a very simple form since the dominant part of P_1 satisfies (43) and almost all escaping probability from region (1) goes to region (2). We can write P_2 as

$$\frac{\mathrm{d}P_2}{\mathrm{d}t} = F_{\mathrm{in}} + F_{\mathrm{out}}, \tag{47}$$

where F_{in} is the probability inflow from region (1) to region (2) and F_{out} is the probability outflow from region (2) to region (3).

F_{in} is simply $\gamma_g\,\mathrm{e}^{-\gamma_g t}$, which is $P_1(t)$ outflow from region (1). For the form of outflow F_{out}, we try an exponential decay model. In that case, F_{out} is set as $-\gamma_{23}P_2$, where γ_{23} is the decay constant from region (2) to region (3). With this assumption, the solution of (47) has the form

$$P_2(t) = \frac{\gamma_g}{\gamma_g - \gamma_{23}}(\mathrm{e}^{-\gamma_{23}t} - \mathrm{e}^{-\gamma_g t}). \tag{48}$$

The decay constant γ_{23} is yet undetermined, so (48) becomes a one parameter fitting model. This exponential decay model of F_{out} implies that the remaining particle in the trap will decay exponentially like one particle decays after the other one escapes, with only one decay mode.

Compared with numerical simulation, model (48) shows very good agreement. Furthermore, it shows that even for larger g, the fitted parameter γ_{23} is very close to the lowest single-particle decay rate γ_{z0}. Figure 5 shows the comparison between numerical simulation and (48) with γ_{23} substituted by γ_{z0} (dashed red line) and (48) with γ_{23} obtained from fitting (blue line), for $g = 0, 1, 10$. All show very good agreement and blue lines are not shown well due to overlapping with red lines. The agreement for even $g = 10$ is quite surprising, since for $g = 10$ the initial wavevectors inside the trap are far from the lowest decay modes, as shown in figure 2. The initial two wavevectors are $k_{1i} = 5.347$ and $k_{2i} = 2.720$, the escaping complex eigenvectors are $k_{1g} = 4.996 - 0.1445\,\mathrm{i}$ and $k_{2g} = 2.507 - 0.048\,81\,\mathrm{i}$ (up to four significant digits) for $g = 10$. k_{1i} and k_{1g} are closer to the second decay mode, but still P_2 decay to region (3) is dominated by the lowest single-particle decay rate. Figure 6 shows γ_{23} compared to γ_{z0} and their relative differences for various g. It shows that the relative difference between γ_{23} and γ_{z0} is less than 2% for $0 < g < 17$, and the difference increases and approaches 10% for larger g.

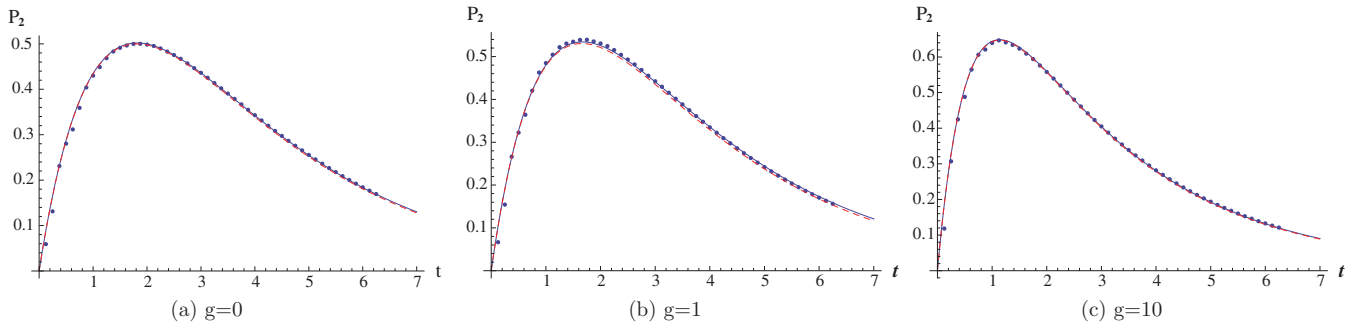

Figure 5. $P_2(t)$ plots from (48) (line) and numerical simulation (dots) for $g = 0, 1, 10$. Dots represent $P_2(t)$ from numerical simulation, dashed red lines are from (48) with γ_{23} is substituted by the lowest decay rate of single particle and blue lines are from (48) with γ_{23} obtained from fitting. All three show very good agreement and lines are almost overlapping.

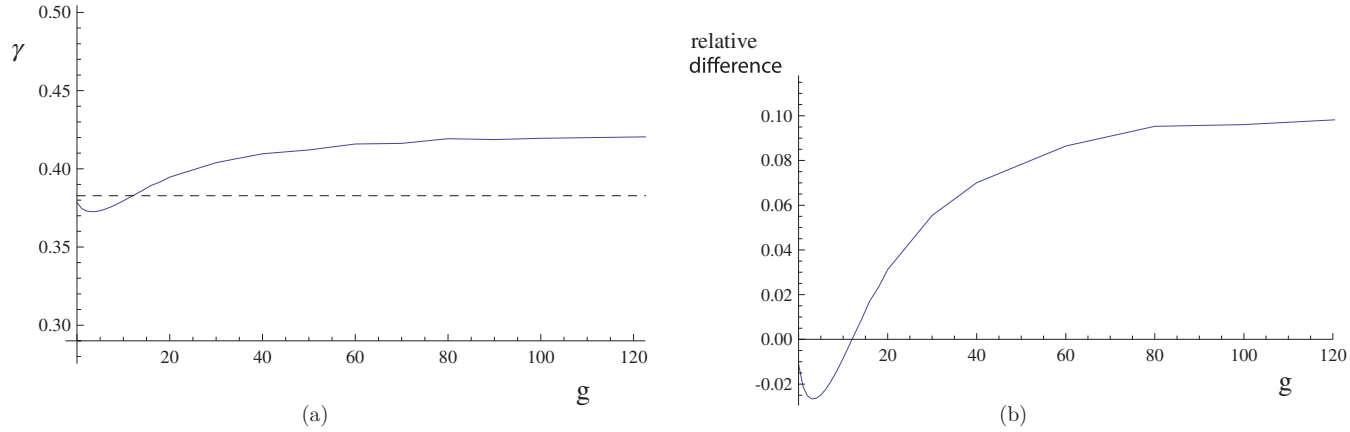

Figure 6. (a) The fitted decay rate γ_{23} (solid line) and the lowest single-particle decay rate γ_{z0} (dashed line) versus g. (b) The relative difference $(\gamma_{23} - \gamma_{z0})/\gamma_{z0}$.

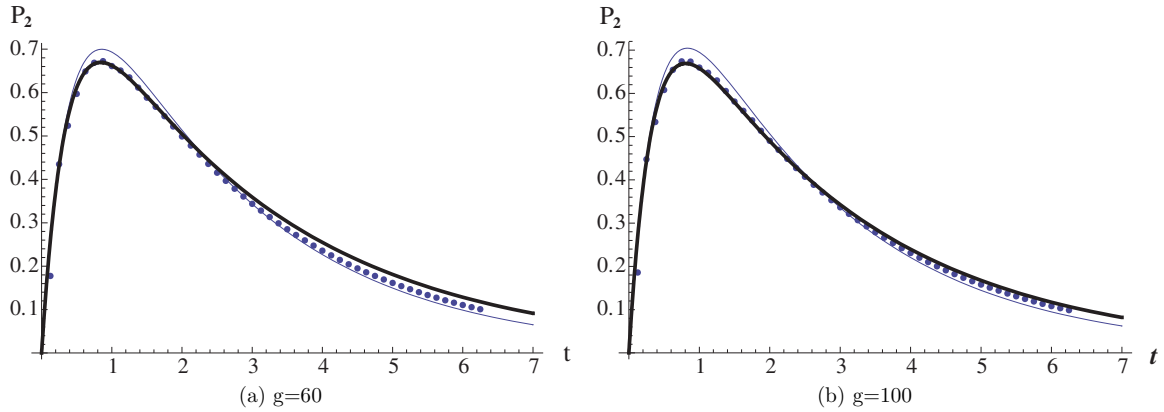

Figure 7. Comparison between numerical simulation (dots) and theoretical models. The black line represents model (49) and the blue line represents model (48). Model (49) shows better agreement with the numerical simulation for larger g.

In the strongly repulsive interaction region where the difference between γ_{23} and γ_{z0} increases, the deviation of model (48) from numerical simulation also increases. In this region we try a different model which is close to (46). The physical meaning of (46) is that there are two decay modes that decay independently without interfering. In our case, we have two complex eigenvectors k_{1g} and k_{2g} from (41) and (42). Assuming that P_2 decays from each complex wavevector and each mode does not interfere with each other, we write the decay model of $P_2(t)$ for large g as

$$P_2(t) = e^{-\gamma_{1g}t}(1 - e^{-\gamma_{2g}t}) + e^{-\gamma_{2g}t}(1 - e^{-\gamma_{1g}t}), \qquad (49)$$

where

$$\gamma_{1g} = -2k_{1gr}k_{1gi}, \qquad \gamma_{2g} = -2k_{2gr}k_{2gi}. \qquad (50)$$

This model works better for larger g than that of (48) as figure 7 shows. The (49) model describes the peak of the $P_2(t)$

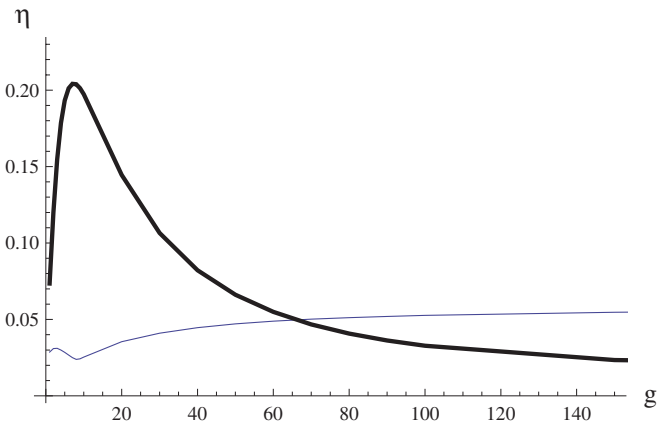

Figure 8. Absolute mean of relative error η plots of model (48) (blue) and model (49) (thick black) versus g.

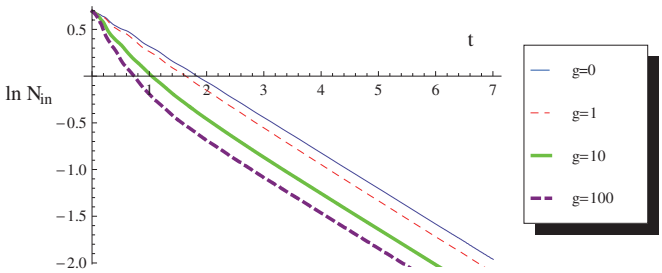

Figure 9. $\ln N_{\rm in}(t)$ plots. For smaller g, it is closer to the straight line (exponential decay) but for larger g the decay rate changes from faster to slower ones.

well, and the discrepancy with the numerical data becomes smaller for larger g.

To see the agreement between the numerical simulation and the fitting model quantitatively, we consider the absolute mean of the relative error η between the probability calculated by the numerical simulation $P_{2\rm num}$ and the probability calculated by the model $P_{2\rm model}$, defined as

$$\eta = \frac{1}{N}\sum_{i}^{N}\frac{|P_{2\rm num}(t_i) - P_{2\rm model}(t_i)|}{P_{2\rm num}(t_i)} \tag{51}$$

with t_is taken from $t = 0.1$ to 5 by 0.1 intervals.

Figure 8 shows that plots of η versus interaction strength g for two different models. Model (48) shows good agreement with the simulation up to $g = 17$, with relative error less than 3%. The error increases steadily, reaching more than 5% when $g > 60$ (seen from figure 2, this is a strongly repulsive region). Model (49) shows large deviation from the numerical simulation for smaller g, but the agreement with the simulation becomes better than that of the (48) model for $g > 67$.

Finally, the probability of both particles outside, P_3, is easily calculated since $P_1 + P_2 + P_3 = 1$. So the total decay mechanism can be described by (43), (48) or (49).

If we calculate the number density $N_{\rm in}(t)$ inside the potential, it is written as

$$N_{\rm in}(t) = \int_{\rm in} {\rm d}x \int {\rm d}x_1\, {\rm d}x_2 \psi^*(x_1, x_2, t) \times \sum_{i=1}^{2}\delta(x - x_i)\psi(x_1, x_2, t) \tag{52}$$

and in our case it simply becomes $N_{\rm in}(t) = 2P_1(t) + P_2(t)$. Figure 9 shows the logarithm of $N_{\rm in}$ versus time. For $g = 0, 1$ the decay of $N_{\rm in}(t)$ is close to exponential ($\ln N_{\rm in}$ close to the straight line) but for larger g it is more visible that the decay rate changes from faster to slower, as expected.

5. Conclusion

We have calculated the decay of two repulsively interacting bosons, initially in the ground state of a potential trap, by numerical simulation. We have found an exponential decay mode for the probability of both bosons inside the trap and have estimated its decay rate theoretically. By applying the outgoing boundary condition for the loss of a single particle from the trap, we obtain two complex wavevectors corresponding to the two particles inside the trap and the corresponding decay rate. The agreement between numerical simulation and theoretical estimation in time evolution of decay probabilities is very good. For describing the probability to have one particle inside and another one outside, two simple models were proposed. For small and moderate g, we apply a model in which the remaining particle decays exponentially, whereas for larger g (strongly repulsive) we propose another model in which the modes of each complex wavevector decay separately. Our numerical simulations show very good agreement for weak and moderate interactions with the first model. For stronger interactions, where fermionization effects become relevant, a separate exponential decay model becomes necessary and agrees well with simulations. The number density shows that the decay rate changes over time from fast to slower decay for large g. The results show that simple models describe the overall decay mechanism of repulsively interacting bosons well.

Acknowledgments

The authors thank A Dudarev for helpful discussions. JB was supported by the Marsden Fund Council (contract no MAU0706) from Government funding administered by the Royal Society of New Zealand.

References

[1] Anderson B P and Kasevich M A 1998 *Science* **282** 1686–9
[2] Leggett A J 2001 *Rev. Mod. Phys.* **73** 307–56
[3] Anderson M H, Ensher J R, Matthews M R, Wieman C E and Cornell E A 1995 *Science* **269** 198–201
[4] Meyrath T P, Schreck F, Hanssen J L, Chuu C-S and Raizen M G 2005 *Opt. Express* **13** 2843–51
[5] Meyrath T P, Schreck F, Hanssen J L, Chuu C-S and Raizen M G 2005 *Phys. Rev.* A **71** 041604
[6] Gross E P 1961 *Il Nuovo Cimento* **20** 454–7
[7] Pitaevskii L P 1961 *Sov. Phys.—JETP* **13** 451–4

[8] Pethick C J and Smith H 2002 *Bose–Einstein Condensation in Dilute Gases* (Cambridge: Cambridge University Press)
[9] Moiseyev N, Carr L D, Malomed B A and Band Y B 2004 *J. Phys. B: At. Mol. Opt. Phys.* **37** L193–200
[10] Moiseyev N and Cederbaum L S 2005 *Phys. Rev.* A **72** 033605
[11] Fleurov V and Soffer A 2005 *Europhys. Lett.* **72** 287–93
[12] Schlagheck P and Wimberger S 2007 *Appl. Phys.* B **86** 385–90
[13] Carr L D, Holland M J and Malomed B A 2005 *J. Phys. B: At. Mol. Opt. Phys.* **38** 3217–31
[14] Fölling S *et al* 2007 *Nature* **448** 1029–32
[15] Zöllner S, Meyer H and Schmelcher P 2008 *Phys. Rev. Lett.* **100** 040401
[16] Öttl A, Ritter S, Köhl M and Esslinger T 2005 *Phys. Rev. Lett.* **95** 090404
[17] Girardeau M 1960 *J. Math. Phys.* **1** 516–23
[18] del Campo A, Delgado F, García-Calderón G, Muga J G and Raizen M G 2006 *Phys. Rev.* A **74** 013605
[19] Lode A U J, Streltsov A I, Alon O E, Meyer H D and Cederbaum L S 2009 *J. Phys. B: At. Mol. Opt. Phys.* **42** 044018
[20] Gaudin M 1971 *Phys. Rev.* A **4** 386–94
[21] Puzynin I V, Selin A V and Vinitsky S I 1999 *Comput. Phys. Commun.* **123** 1–6
[22] Mişicu S, Rizea M and Greiner W 2001 *J. Phys. G: Nucl. Part. Phys.* **27** 993–1003